

## Modal analysis of perforated rectangular plates in contact with water

Kyeong-Hoon Jeong<sup>†</sup>

*Korea Atomic Energy Research Institute, P.O. Box 105, Yusong, Taejeon 305-600, Korea*

Byung-Ki Ahn<sup>‡</sup> and Seong-Cheol Lee<sup>‡‡</sup>

*Department of Mechanical Engineering, Chonbuk National University, Chonju, Chonbuk 560-756, Korea*

**Abstract.** This paper presents an experimental modal analysis of perforated rectangular plates in air or in contact with water. The penetration of holes in the plates had a triangular pattern with  $P/D$  (pitch to diameter) 2.125, 2.500, 3.000 and 3.750. The plate was clamped along the plate edges by a number of bolts and nuts. The natural frequencies of the perforated plates in air were obtained by the analytical method based on the relation between the reference kinetic and maximum potential energies and compared with the experimental results. Good agreement between the results was found for the natural frequencies of the perforated plates in air. Additionally, it was empirically found that the natural frequencies of the perforated plate in air increase with an increase of  $P/D$ , on the other hand, the natural frequencies of the perforated plate in contact with water decrease with an increase of  $P/D$ .

**Key words:** experimental modal analysis; fluid-structure interaction; perforated plate; added mass; clamped boundary condition; rectangular plate; triangular hole pattern; natural frequency; free vibration.

---

### 1. Introduction

This paper deals with the free vibration analysis of a perforated rectangular plate in air or in contact with water bounded by rigid walls. The work arises as part of a project investigating the free vibration of a flow distribution plate in an integral reactor. The flow distribution plate, as a thin perforated circular plate in contact with coolant, is installed into the reactor in order to provide a means of distributing inlet coolant flow to the core. This study investigating the dynamic characteristics of a perforated plate in contact with fluid was carried out as a basic study for the flow distribution plate.

Free vibration of plates in contact with fluid has recently been studied. Kwak (1991, 1997), Kwak and Han (2000), Kwak and Kim (1991), and Amabili and Kwak (1996, 1999a) studied the free vibration of a circular plate in contact with water on one side, while the free vibration of an annular plate in contact with water on one side was investigated by Amabili *et al.* (1996) and Amabili and Kwak (1999b). They considered the fluid-contacting solid plates and introduced the non-

---

<sup>†</sup> Principal Researcher

<sup>‡</sup> Graduate Student

<sup>‡‡</sup> Professor

dimensionalized added virtual mass incremental (NAVMI) factors in order to estimate the fluid effect on the individual natural frequency of the fluid-structure coupled system. Chiba (1994) obtained exact solutions for the circular elastic bottom plate in a cylindrical rigid tank filled with fluid. The elastic bottom plate was supported by an elastic foundation and the free surface of the fluid was considered. Bauer (1995) analytically determined the coupled natural frequencies of an ideal fluid in a cylindrical container where the free fluid surface was covered by a flexible membrane or an elastic plate. Montero de Espinosa *et al.* (1984) studied the vibration of plates submerged in water mainly to the lower modes by the approximate analytical method and experiments. Hagedorn (1994) dealt with the theoretical free vibrations of an infinite elastic plate in the presence of water. Jeong (1998) studied the free vibration of two identical circular plates coupled with fluid. An experimental modal analysis of perforated circular plates submerged in water was carried out (De Santo 1981). However, the holes in the plate were too large to use equivalent material properties. However, all of these works are concerned with circular plates.

On the other hand, there are relatively few available theoretical results on the free vibration of rectangular plates in contact with water. The effect of supporting boundary conditions of plates was studied and the experimental results were verified by their theoretical results (Kim *et al.* 1978, 1979). Fu and Price (1987) investigated the vibration of a cantilever plate partially or fully immersed in water. Muthuverappan *et al.* also studied the free vibration of a cantilever square plate (1978) and a cantilever rectangular plate (1979) immersed in water, and they investigated the effect of boundary conditions of the plate on the added mass of fluid (1980) using the finite element method. The finite element displacement method for a modal analysis of a plate in contact with fluid was developed (Hori *et al.* 1994). Kwak (1996) theoretically obtained the natural frequencies of a rectangular plate floating on a fluid and compared with the experimental results obtained (Kim *et al.* 1979).

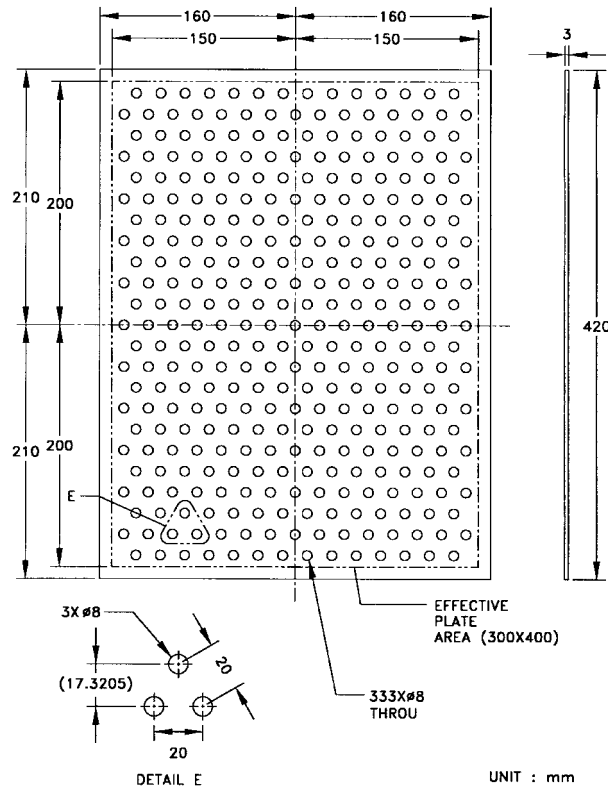
However, these studies on a solid plate in contact with fluid cannot predict the dynamic characteristics of the perforated plate in contact with water. Thus, this paper is concerned with the coupling effect of contacting fluid on the free vibration characteristics of a perforated rectangular plate supported by rigid walls filled with water. The plates with a number of holes are clamped along the edges of the plate. The natural frequencies of the plate in air are obtained from the theoretical calculation and the experiment. Additionally, a formulation for the natural frequencies of the fluid-coupled system is shown to be difficult, and the natural frequencies and mode shapes of the fluid-coupled perforated plate with a number of circular holes are obtained by the experiment.

## 2. Theoretical background

### 2.1 Equation of motion of a perforated rectangular plate

Fig. 1 represents a perforated rectangular plate in contact with water, where  $a$ ,  $b$  and  $h$  represent the width, length and thickness of the plate, respectively. The following assumptions are made: (a) the water motion is small; (b) the water motion is incompressible, inviscid and irrotational; (c) the perforated plate is made of linearly elastic, homogeneous, and isotropic material; (d) the shear deformation and rotary inertia are negligible; and (e) the thickness of the plate is very thin compared to the width and the length.

The simplified design methods were developed for analyzing stress and transverse deflection in

Fig. 1 A typical perforated rectangular plate with  $P/D=2.500$ 

plates perforated with a large number of holes arranged in an equilateral array. Such plates can be treated as isotropic homogeneous continua where effective elastic constants are used to account for the effect of the holes on the stiffness and density of the plate. The perforated plate can be replaced by a solid plate with modified effective elastic constants such as the effective density  $\rho^*$ , the effective Poisson's ratio  $\mu^*$  and the effective elastic modulus of the plate  $E^*$ . The effective elastic constants for the perforated plates used in the experiment were obtained by the interpolation method based on the tables of O'Donnell *et al.* (1962) and Slot *et al.* (1971), which are listed in Table 1.

When the perforated rectangular plate is in contact with an ideal fluid as shown in Fig. 1, the equation of motion for transverse displacement,  $w$ , of the plates is:

Table 1 Equivalent material properties of the perforated plates

| Pitch<br>(mm) | $P/D$ | Ligament<br>efficiency,<br>$\eta$ | Equivalent<br>Poisson's ratio,<br>$\mu^*$ | Equivalent Young's<br>modulus,<br>$E^*$ , (GPa) | Equivalent<br>mass density<br>$\rho^*$ , (kg/m <sup>3</sup> ) |
|---------------|-------|-----------------------------------|---|---|---|
| 17            | 2.125 | 0.5294                            | 0.3182                                    | 39.26   | 2157.7  |
| 20            | 2.500 | 0.6000                            | 0.3154                                    | 45.85   | 2308.2  |
| 24            | 3.000 | 0.6667                            | 0.3105                                    | 51.60   | 2427.9  |
| 30            | 3.750 | 0.7333                            | 0.3042                                    | 56.67   | 2525.9  |

$$\nabla^4 w + \frac{\rho^* h}{D^*} \frac{\partial^2 w}{\partial t^2} = \frac{p^*}{D^*} \quad (1)$$

where  $D^* = E^* h^3 / 12(1 - \mu^{*2})$  is the effective flexural rigidity of the perforated plate and  $p^*$  is the hydrodynamic pressure on the perforated plate. The effective elastic constants of the plate depend upon the pitch to diameter ( $P/D$ ) of the holes in the plate. In addition,

$$\nabla^4 = \frac{\partial^4}{\partial x^4} + 2 \frac{\partial^4}{\partial x^2 \partial y^2} + \frac{\partial^4}{\partial y^4} \quad (2)$$

is the bihamonic operator in Cartesian coordinates  $x$  and  $y$ . The general solution of Eq. (1) can be written as

$$w(x, y, t) = W_{mn}(x, y) \exp(i \omega_f t), \quad (3)$$

where,  $i = \sqrt{-1}$  and  $\omega_f$  means the natural frequency of the plate in contact with water. A general closed-form solution does not exist for the free vibration of a rectangular plate with the clamped edge boundary condition. However, it has been found that the mode shapes of the plate can be well approximated by the beam modes in the separation form of the variables:

$$W_{mn}(x, y) = A_{mn} U_m(x) V_n(y) \quad (4)$$

where,  $W_{mn}(x, y)$  is the  $m$ - $n$  mode shape of the plate and  $A_{mn}$  is the modal constant. The admissible functions,  $U_m(x)$  and  $V_n(y)$  are the beam mode shapes which satisfy the appropriate boundary conditions on edges  $y=0, b$  and  $x=0, a$ , respectively. Therefore, the dynamic transverse displacement of the plates can be assumed for the clamped edges:

$$W_{mn}(x, y) = A_{mn} \left[ \cosh\left(\frac{\lambda_m x}{a}\right) - \cos\left(\frac{\lambda_m x}{a}\right) - \sigma_m \left\{ \sinh\left(\frac{\lambda_m x}{a}\right) - \sin\left(\frac{\lambda_m x}{a}\right) \right\} \right] \\ \times \left[ \cosh\left(\frac{\lambda_n y}{b}\right) - \cos\left(\frac{\lambda_n y}{b}\right) - \sigma_n \left\{ \sinh\left(\frac{\lambda_n y}{b}\right) - \sin\left(\frac{\lambda_n y}{b}\right) \right\} \right], \quad (5)$$

in which  $m$  and  $n$  are the number of modes. The coefficients, when  $j=1, 2, 3, \dots$ ,  $\lambda_j = 4.73004, 7.85320, 10.99561, 14.13717, 17.27876, (2j+1)\pi/2 (j>5)$  and  $\sigma_j = 0.98250, 1.00078, 0.99997, 1.00000 (j>3)$ , where  $j$  will be  $n$  or  $m$ .

## 2.2 Velocity potential

Next consider the water region with which the perforated rectangular plate and the rigid container walls are surrounded. When water is assumed as an ideal fluid, the three-dimensional oscillatory fluid flow can be described with the velocity potential. The bottom surface of the rectangular plate is in contact with water and the top surface of the plate is exposed to air. The fluid movement due to vibration of the plate can be described using the spatial velocity potential that satisfies Laplace

equation:

$$\nabla^2 \Phi(x, y, z, t) = 0 \quad (6)$$

It is possible to separate the velocity potential function  $\Phi$  with respect to  $x$  and  $y$  by observing that the container supports the edges of the plates that are assumed to be rigid, as in the case of the complete contact rectangular plate. The general velocity potential  $\Phi$  can be expressed as a combination of the spatial velocity potential  $\phi$  and a harmonic time function.

$$\Phi(x, y, z, t) = i \omega_f \phi(x, y, z) \exp(i \omega_f t) \quad (7)$$

The boundary conditions along the rigid container wall that assure a zero fluid velocity, are given by:

$$\left( \frac{\partial \phi}{\partial x} \right)_{x=0} = \left( \frac{\partial \phi}{\partial x} \right)_{x=a} = 0 \text{ at } x=0 \text{ and } x=a \text{ of the rigid container wall,} \quad (8)$$

$$\left( \frac{\partial \phi}{\partial y} \right)_{y=0} = \left( \frac{\partial \phi}{\partial y} \right)_{y=b} = 0 \text{ at } y=0 \text{ and } y=b \text{ of the rigid container wall,} \quad (9)$$

$$\left( \frac{\partial \phi}{\partial z} \right)_{z=-d} = 0 \text{ at } z=-d \text{ of the rigid container bottom} \quad (10)$$

### 2.3 Natural frequencies of a perforated rectangular plate

The reference kinetic and strain energies of the perforated plate can be given using the effective elastic constants,  $\rho^*$ ,  $D^*$  and  $\mu^*$  as shown in the total energy expressions for the solid plate.

$$T_d = \frac{1}{2} \rho^* h \int_0^a \int_0^b W_{mn}^2 dx dy, \quad (11)$$

$$V_p = \frac{D^*}{2} \int_0^a \int_0^b \left[ \left( \frac{\partial^2 W_{mn}}{\partial x^2} \right)^2 + \left( \frac{\partial^2 W_{mn}}{\partial y^2} \right)^2 + 2 \mu^* \frac{\partial^2 W_{mn}}{\partial x^2} \frac{\partial^2 W_{mn}}{\partial y^2} + 2(1 - \mu^*) \left( \frac{\partial^2 W_{mn}}{\partial x \partial y} \right)^2 \right] dx dy \quad (12)$$

The natural frequency of the perforated plate in air can then be written

$$\omega = \sqrt{V_p / T_d} \quad (13)$$

In order to get the reference kinetic energy of water, the velocity potential satisfying the boundary and compatibility conditions must be obtained. The compatibility condition along the water interfacing with the rectangular plate yields;

$$W_{mn} = - \left( \frac{\partial \phi}{\partial z} \right)_{z=0} \text{ at the solid boundary,} \quad (15)$$

$$\phi|_{z=0} = 0 \text{ at the holes of the plate.} \quad (16)$$

That is to say, Eq. (15) is only applicable to the solid part of the plate, on the other hand, the fluid has the free surface at the plate holes as described in Eq. (16). So it is very difficult to theoretically describe fluid motion at the interfacing boundary between the plate and the fluid. It is necessary to know the reference kinetic energies of the containing water in order to calculate the coupled natural frequency of the perforated rectangular plate. By using the hypothesis of irrotational movement of water, the reference kinetic energy of water can be evaluated from its boundary motion. In fact, as a consequence of Green's theorem applied to the harmonic function  $w$ , additionally the functions  $\partial\phi/\partial x$  and  $\partial\phi/\partial y$  are always zero on the boundary of water, except the surface in contact with the plate and the free surface at  $z=0$ , one obtains

$$T_F = \frac{1}{2} \rho_0 \int_0^a \int_0^b \left( \frac{\partial\phi(x,y,z)}{\partial z} \right)_{z=0} \phi(x,y,0) dx dy. \quad (17)$$

If the mode shapes in air and in contact with water are assumed to be identical, the coupled natural frequency of the rectangular perforated plate in contact with water can be related to the natural frequency in air,  $\omega$ ,

$$\omega_f = \frac{\omega}{\sqrt{1 + T_F/T_d}}. \quad (18)$$

Unfortunately, it is impossible to find the closed form of velocity potential satisfying Laplace equation, Eq. (6), the boundary conditions of Eqs. (8)-(10) and the compatibility equation of Eqs. (15)-(16) at the same time, because of the complex compatibility condition of Eqs. (15) and (16). Therefore, the coupled natural frequencies of the rectangular perforated plate in contact with water cannot be obtained by the theory.

### 3. Experiments

#### 3.1 Experimental equipment and procedure

An empirical modal test was carried out for several perforated rectangular plates which were made of aluminum to verify the theoretical results in air and to find the hydrodynamic effect on a perforated plate in contact with water. Each perforated rectangular plate had a 300 mm × 400 mm effective area with a 3.0 mm thickness as shown in Fig. 1. A typical perforated plate having the triangular hole pattern with  $P/D$  (pitch to diameter)=2.500 is shown in Fig. 1. The penetration is composed of 8 mm diameter circular holes which had the triangular hole pattern with  $P/D=2.125, 2.500, 3.000$  and  $3.750$ . The perforated plate was clamped using the upper and lower containers with 60 bolts and nuts as shown in Fig. 2. The lower container was made of carbon steel and also has a 300 mm × 400 mm area with a 240 mm depth for water contents. The upper container was made of the same material and had the same area. The two containers had a 10 mm thickness which gave enough stiffness for supporting the perforated aluminum plate. Additionally, twenty bars were welded to the outside walls of the lower container in order to obtain the stiffness large enough to neglect local deformations of the container. Each perforated plate was immersed to half of the plate's thickness in water very carefully for the wet experiment. For embodiment of the clamped

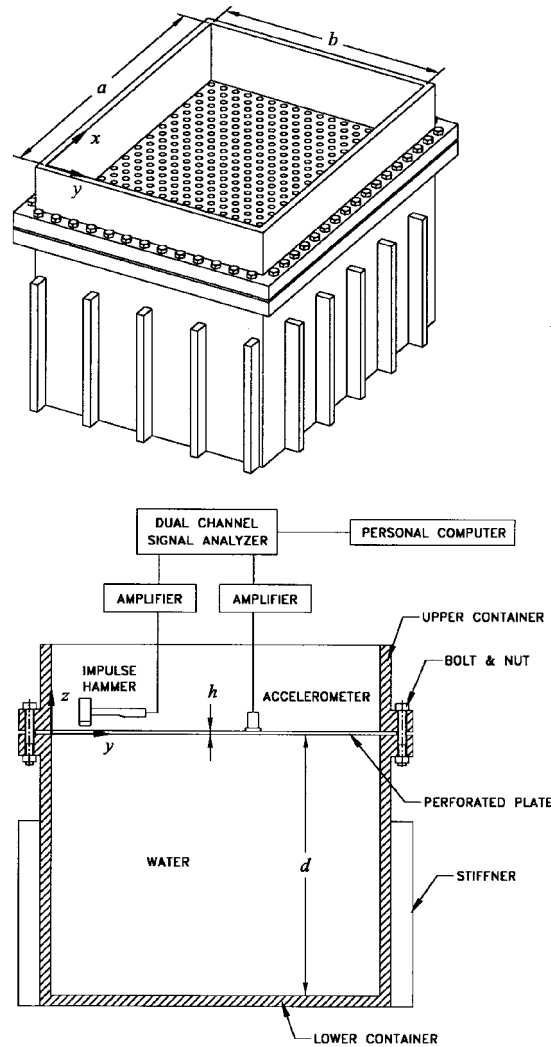


Fig. 2 The experimental setup

boundary condition, the plates were larger than the effective size by 20 mm along the edges. The solid aluminum plates had the following material properties: Young's modulus  $E=69.0$  GPa, Poisson's ratio  $\mu=0.3$ , material density  $\rho=2700$  kg/m<sup>3</sup>.

The experimental setup and equipment are shown in Fig. 2. The experimental modal test was performed by the impulse hammer excitation. The impulse hammer (PCB, 086C03) was used to excite the plate and a small accelerometer (PCB, A353 A17) of 2.5 g was attached to the top surface of the plate. The mass ratio of the accelerometer to the plate with  $P/D=2.125$  is only 0.37%. Hence, for the most severe case with  $P/D=2.125$ , the influence of mass increase due to the accelerometer on the natural frequency is expected to be negligible. In order to acquire a good signal, the excitation point was fixed to the designated point that was not far from the supporting edge, and the accelerometers were moved to the other designated points in turn. The signals from the hammer and the accelerometer were amplified by the amplifier (PCB, 480 E09) and fed into the

Table 2 Natural frequency (Hz) of a solid plate in air

| Method     | Mode number ( $n \times m$ ) |              |              |              |              |              |
|------------|------------------------------|--------------|--------------|--------------|--------------|--------------|
|            | $1 \times 1$                 | $1 \times 2$ | $2 \times 1$ | $1 \times 3$ | $2 \times 2$ | $2 \times 3$ |
| Theory     | 233.7                        | 392.7        | 550.4        | 654.0        | 697.8        | 944.8        |
| FEM        | 232.1                        | 388.6        | 545.3        | 646.3        | 687.0        | 927.1        |
| Experiment | 215.0                        | 365.1        | 509.3        | 622.5        | 656.3        | 898.4        |

Table 3 Natural frequency (Hz) of the perforated plates in air

| $P/D$ | Method     | Mode number ( $n \times m$ ) |              |              |              |              |              |
|-------|------------|------------------------------|--------------|--------------|--------------|--------------|--------------|
|       |            | $1 \times 1$                 | $1 \times 2$ | $2 \times 1$ | $1 \times 3$ | $2 \times 2$ | $2 \times 3$ |
| 2.125 | Theory     | 198.4                        | 333.4        | 467.3        | 555.3        | 593.5        | 802.5        |
|       | Experiment | 189.4                        | 324.2        | 450.9        | 546.3        | 581.5        | 787.2        |
| 2.500 | Theory     | 207.1                        | 348.0        | 487.8        | 579.7        | 618.4        | 837.3        |
|       | Experiment | 193.7                        | 331.5        | 462.9        | 559.1        | 597.9        | 811.8        |
| 3.000 | Theory     | 213.9                        | 359.4        | 503.7        | 598.6        | 638.6        | 864.6        |
|       | Experiment | 197.3                        | 340.8        | 469.2        | 575.7        | 605.5        | 827.4        |
| 3.750 | Theory     | 219.3                        | 368.5        | 516.4        | 613.7        | 654.7        | 886.5        |
|       | Experiment | 204.2                        | 353.3        | 483.6        | 598.2        | 626.4        | 857.7        |

dual channel FFT analyzer (DI, DI2200). The frequency bandwidth was limited to 1.6 kHz. The mode shapes were determined from the quadrature components measured frequency response at 63 ( $7 \times 9$ ) impact locations of the plates. The modal damping values for each individual vibration mode were also obtained using the half power bandwidth method. The natural frequency of a rectangular solid plate in air was also measured, which was compared to the theoretical natural frequency and the results from the finite element analysis using a commercial computer code, ANSYS 5.5 as shown in Table 2. The comparison confirms that the clamped boundary conditions of the plate were realized in the experiment. Table 3 shows the experimental and theoretical natural frequency of the perforated rectangular plates in air. The comparison between them also confirms that the uniform and perfect rectangular perforated plates were manufactured and the appropriate equivalent properties of the plates were selected.

### 3.2 Experimental results and discussion

Table 2 shows the measured and theoretical natural frequency of the solid rectangular plate without a hole when the clamped plate was in air. In the tables,  $m$  is the number of nodal lines in the width of 400 mm and  $n$  is the number of the nodal lines in the length of 300 mm. The theoretical results were obtained by using the assumed mode method based on the clamped beam functions. The natural frequencies obtained by the assumed mode method were overestimated comparing with those by the finite element analysis because the beam functions as admissible functions are not exactly identical to the real mode shapes but just close to the eigenvectors. The closeness of the estimated natural frequencies to the actual values depends on how close the



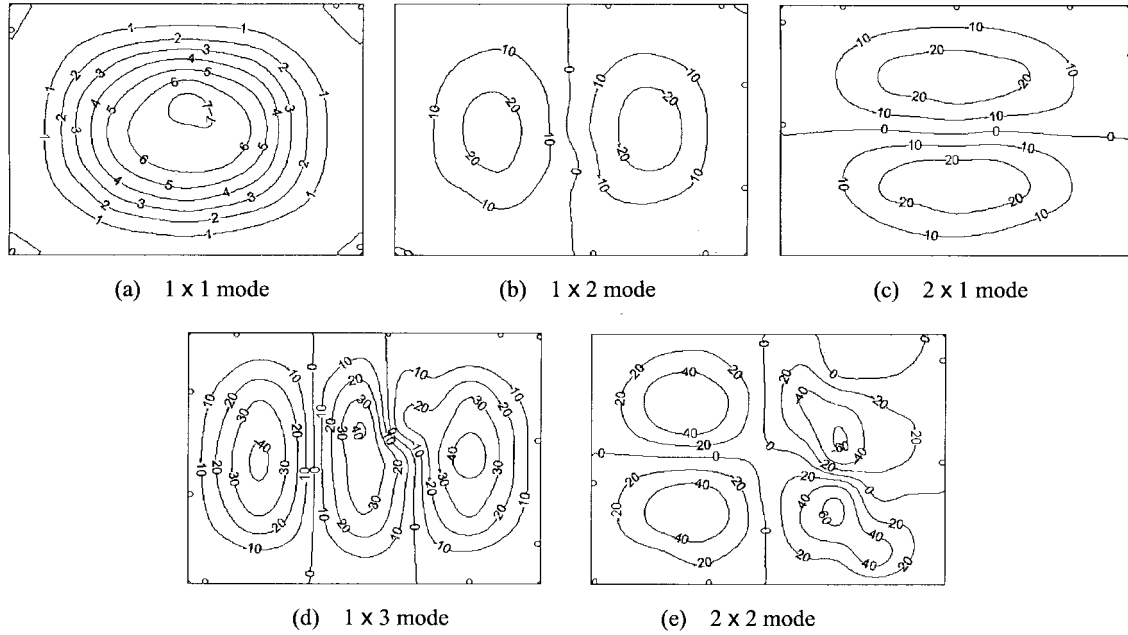
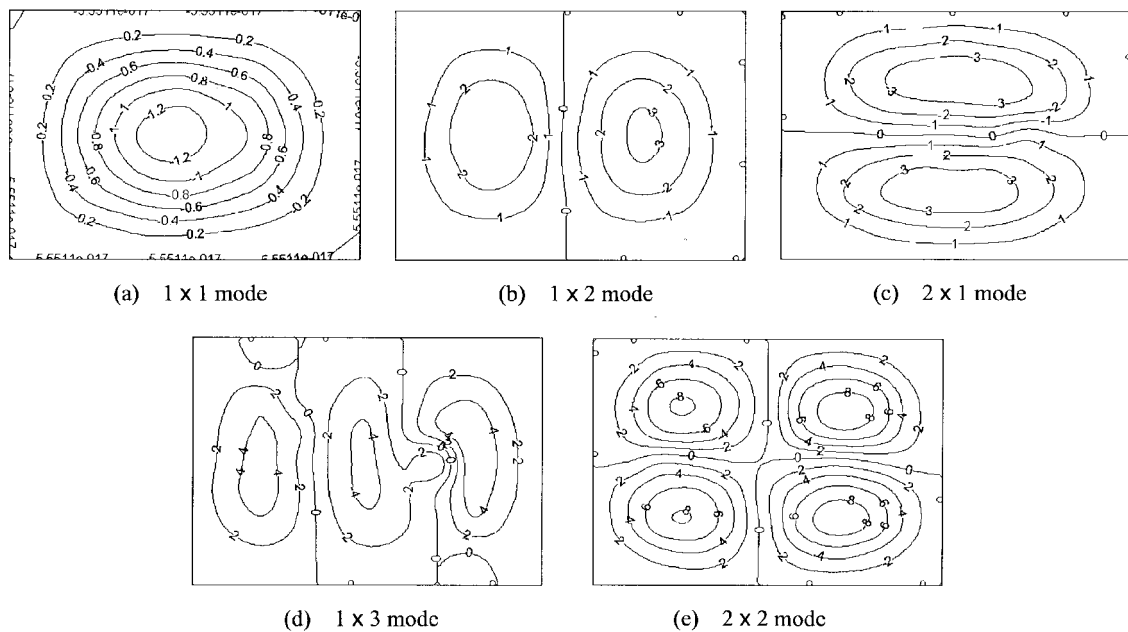
admissible functions are to the real eigenvectors. Generally speaking, as the clamped edge cannot make a perfect zero slope displacement practically in an experiment, it takes for granted that the measured natural frequencies are always less than the theoretical values. Therefore, it is clear that the results of Table 2 are reasonable.

The experimental natural frequencies of the perforated plates were compared with the theoretical ones in Table 3 with respect to the various  $P/D$  values. It was found that the theoretical natural frequencies could predict the measured ones well within an 8.4% deviation. Similarly, owing to the imperfect clamped boundary condition with small deformation in the containers, the theoretical natural frequency was overestimated comparing with the measured ones by about 5%. The theoretical natural frequency based on the assumed mode method was calculated using the equivalent material property estimation suggested by O'Donnell and Langer (1962). As the pitch between the holes in the plate decreases, the natural frequency of the plate in air also reduces, as listed in Table 3. The first measured natural frequency in air, 189.4 Hz when  $P/D=2.125$  increases to 204.2 Hz when  $P/D=3.750$ . The first natural frequency eventually increased to 215.0 Hz in the case of the solid plate. It is possible to say that the rigidity and mass of the plate decrease at the same time, when  $P/D$  decreases. Generally speaking, when a dimensional size of structures is reduced linearly, the mass reduction is proportional to the dimension, however the stiffness reduction is proportional to the cubic of the dimension. Similarly in this case, when the pitch between the holes decreases, the effect of rigidity reduction in the plate is dominant over that of mass reduction. Therefore, the gap between the holes in the plate is reduced, and the natural frequency of the perforated plate in air decreases.

Table 4 shows the effect of fluid on the natural frequency of the perforated plates with clamped edges. As the pitch between the holes in the plate increases, the coupled natural frequencies of the plate in contact with water gradually decreases. The first measured natural frequency in contact with water, 148.1 Hz when  $P/D=2.125$  decreases to 100.5 Hz when  $P/D=3.750$ . From Tables 3 and 4, owing to the added mass of water, the first five natural frequencies in contact with water are less than those in air by about 21% for  $P/D=2.125$ . The natural frequency reduction for  $P/D=3.370$  is up to about 47% as given in Tables 3 and 4. The deviation in the frequency reduction rate can be explained by an increase of the water-contacting area. When the hole pitch in the plate decreases, the water-contacting area decreases. So the hydrodynamic mass effect on the plate vibration is also reduced. Eventually, the hydrodynamic mass reduction provides the decrease of natural frequency according to the pitch reduction. Moreover, by decreasing  $P/D$ , the free surface area of water increases and the water movement is less constraint by the perforated plate. These effects increase the natural frequency of the plate coupled with water as a consequence that decrease the added mass effect of water. The dry and wet mode shapes of the perforated plate with  $P/D=2.500$  are

Table 4 Experimental natural frequency (Hz) of the perforated plates in contact with water

| $P/D$ | Mode number ( $n \times m$ ) |              |              |              |              |
|-------|------------------------------|--------------|--------------|--------------|--------------|
|       | $1 \times 1$                 | $1 \times 2$ | $2 \times 1$ | $1 \times 3$ | $2 \times 2$ |
| 2.125 | 148.1                        | 254.2        | 355.7        | 426.8        | 452.7        |
| 2.500 | 129.1                        | 228.1        | 313.1        | 385.7        | 415.8        |
| 3.000 | 114.5                        | 204.7        | 278.3        | 356.6        | 368.2        |
| 3.750 | 100.5                        | 186.4        | 269.5        | 322.5        | 347.4        |

Fig. 3 Experimental mode shapes of the perforated plate in air ( $P=20$  mm)Fig. 4 Experimental mode shapes of perforated plate in contact with water ( $P=20$  mm)

shown in Fig. 3 and Fig. 4, respectively. It is shown that there is no big difference between the two corresponding mode shapes. Some distorted mode shapes were detected because of non-uniformity of the holes. The modal damping values of each mode are listed in Table 5. The modal damping of

Table 5 Damping ratio (%) of the perforated plates

|     | $P/D$ | Mode number ( $n \times m$ ) |              |              |              |              |
|-----|-------|------------------------------|--------------|--------------|--------------|--------------|
|     |       | $1 \times 1$                 | $1 \times 2$ | $2 \times 1$ | $1 \times 3$ | $2 \times 2$ |
| Dry | 2.125 | 7.13                         | 3.45         | 4.35         | 1.79         | –            |
|     | 2.500 | 4.62                         | 3.19         | 2.61         | 2.51         | 1.31         |
|     | 3.000 | 4.31                         | 8.13         | 2.01         | 1.88         | 3.85         |
|     | 3.750 | 5.42                         | 2.46         | 2.87         | 1.32         | –            |
| Wet | 2.125 | 18.12                        | 7.78         | 8.73         | 6.73         | 5.17         |
|     | 2.500 | 8.68                         | 10.89        | 11.12        | 8.85         | 7.03         |
|     | 3.000 | 12.53                        | 13.10        | 11.09        | 4.69         | –            |
|     | 3.750 | 8.31                         | 5.81         | 4.59         | 7.02         | 3.81         |

the perforated plates in contact with water is greater than that of plates in air due to fluid damping.

#### 4. Conclusions

An experimental study for evaluating the linear free vibration of thin-walled perforated rectangular plates in contact with water was carried out. The analytical method for the dry modes was developed under the assumption of a clamped boundary condition along the plate edges. The results show that the calculated natural frequency in air can predict the measured ones well. It is theoretically and experimentally found that the natural frequency of the perforated plates in air increases with increasing  $P/D$  because the rigidity increase of the plates is dominant comparing with the increase of structural mass. On the other hand, the natural frequency of the perforated plates in contact with water decreases with increasing  $P/D$  because the added mass increases due to an increase in the fluid-contacting area and, mainly, to the reduction of the free surface area of water. Experiments for the submerged perforated plates into water are included in future research plans for investigating the hydrodynamic coupling effect of perforated plates.

#### References

- Amabili, M., Frosali, G., and Kwak, M.K. (1996), "Free vibrations of annular plates coupled with fluids", *J. Sound and Vibration*, **191**, 825-846.
- Amabili, M., and Kwak, M.K. (1996), "Free vibrations of circular plates coupled with liquids: Revising the lamb problem", *J. Fluids and Structures*, **10**, 743-761.
- Amabili, M., and Kwak, M.K. (1999a), "Vibrations of circular plates on a free fluid surface: effect of surface waves", *J. Sound and Vibration*, **226**, 407-424.
- Amabili, M., and Kwak, M.K. (1999b), "Hydroelastic vibrations of free-edge annular plates", *J. Vibration and Acoustics, Transactions of the ASME*, **121**, 26-32.
- Bauer, H.F. (1995), "Coupled frequencies of a liquid in a circular cylindrical container with elastic liquid surface cover", *J. Sound and Vibration*, **180**, 689-704.
- Chiba, M. (1994), "Axisymmetric free hydro-elastic vibration of a flexural bottom plate in a cylindrical tank supported on an elastic foundation", *J. Sound and Vibration*, **169**, 387-394.

- De Santo, D.F. (1981), "Added mass and hydrodynamic damping of perforated plates vibrating in water", *J. Pressure Vessel Technology, Transactions of the ASME*, **103**, 175-182.
- Fu, Y., and Price, W.G. (1987), "Interaction between a partially or totally immersed vibrating cantilever plate and the surrounding fluid", *J. Sound and Vibration*, **118**, 495-513.
- Hagedorn, P. (1994), "A note on the vibrations of infinite elastic plates in contact with water", *J. Sound and Vibration*, **175**, 233-240.
- Hori, Y., Kanoi, M., and Fujisawa, F. (1994), "Two dimensional coupling vibration analysis of fluid and structure using FEM displacement method," *J. Society of Mechanical Engineers of Japan*, **C60**, 1-7 (in Japanese).
- Jeong, K.H., Kim, T.W., Choi, S., and Park, K.B. (1998), "Free vibration of two circular disks coupled with fluid", *ASME/JSME Joint Pressure Vessels and Piping Conference*, San Diego, U.S.A. July 26-30, 1998.
- Kim, K.C., and Kim, J.S. (1978), "The effect of the boundary condition on the added mass of a rectangular plate," *J. Society of Naval Architects of Korea*, **15**, 1-11 (in Korean).
- Kim, K.C., Kim, J.S., and Lee, H.Y. (1979), "An experimental study on the elastic vibration of plates in contact with water," *J. Society of Naval Architects of Korea*, **16**, 1-7 (in Korean).
- Kwak, M.K. (1991), "Vibration of circular plates in contact with water", *J. Appl. Mech., Transactions of the ASME*, **58**, 480-483.
- Kwak, M.K. (1996), "Hydroelastic vibration of rectangular plates", *J. Appl. Mech., Transactions of the ASME*, **63**, 110-115.
- Kwak, M.K. (1997), "Hydroelastic vibration of circular plates", *J. Sound and Vibration*, **201**, 293-303.
- Kwak, M.K. and Kim, K.C. (1991), "Axisymmetric vibration of circular plates in contact with fluid", *J. Sound and Vibration*, **146**, 381-389.
- Kwak, M.K., and Han, S.B. (2000), "Effect of fluid depth on the hydroelastic vibration of free-edge circular plate", *J. Sound and Vibration*, **230**, 171-185.
- Lee, H.S., and Kim, K.C. (1984), "Transverse vibration of rectangular plates having an inner cutout in water," *J. Society of Naval Architects of Korea*, **21**, 21-34 (in Korean).
- Meylan, M.H. (1997), "The forced vibration of a thin plate floating on an infinite liquid", *J. Sound and Vibration*, **205**, 581-591.
- Montero de Espinosa, F., and Gallego-Zuarez, J.A. (1984), "On the resonance frequencies of water-loaded circular plate", *J. Sound and Vibration*, **94**, 217-222.
- Muthuveerappan, G., Ganesan, N., and Veluswami, M.A. (1978), "Vibration of square cantilever plate immersed in water", *Letters to the editor, J. Sound and Vibration*, **61**, 467-470.
- Muthuveerappan, G., Ganesan, N., and Veluswami, M.A. (1979), "A note on vibration of a cantilever plate immersed in water", *J. Sound and Vibration*, **63**, 358-391.
- Muthuveerappan, G., Ganesan, N., and Veluswami, M.A. (1980), "Influence of fluid added mass on the vibration characteristics of plates under various boundary conditions", *Letters to the editor, J. Sound and Vibration*, **69**, 612-615.
- O'Donnell, W.J. and Langer, B.F. (1962), "Design of perforated plates", *J. Eng. Industry, Transactions of the ASME*, 307-318.
- Slot, T., and O'Donnell, W.J. (1971), "Effective elastic constants for thick perforated plates with square and triangular penetration patterns," *J. Eng. for Industry, Transactions of the ASME*, 935-942.